

Inclined layer Soret instabilities

A. Zebib^{1,2,*} and M. M. Bou-Ali²

¹*Mechanical and Aerospace Engineering, Rutgers University, Piscataway, New Jersey 08854, USA*

²*Department of Manufacturing, Mondragon University, 20500 Mondragon, Spain*

(Received 16 February 2009; published 8 May 2009)

Linear stability of a binary mixture buoyant return flow in a differentially heated inclined infinite layer is investigated by asymptotic long-wave analysis and pseudospectral Chebyshev numerical solutions. The Soret coefficient is negative so that thermodiffusion separates the species with the heavier component migrating to the hot wall, thus, promoting unstable stratification except in the classical Rayleigh-Benard arrangement. It is shown that longitudinal instabilities with small wave numbers are triggered at any finite temperature difference at all angles of inclination except very close to the horizontal heated from the above or below arrangements. Numerical results are given for a specific water-ethanol mixture and are in excellent agreement with the asymptotic results. As is well known the heated from below horizontal layer is overstable while that heated from above is doubly-diffusive unstable. Transition from the longitudinal stationary instabilities in inclined layers to these instabilities in horizontal layers is also given for this mixture.

DOI: [10.1103/PhysRevE.79.056305](https://doi.org/10.1103/PhysRevE.79.056305)

PACS number(s): 47.20.Bp, 66.10.cd, 47.57.eb

I. INTRODUCTION

Differentially heated layer convective instabilities have been the subject of many studies not only because of its importance in geophysics and technological applications but also because it serves as a paradigm for pattern formation and symmetry-breaking bifurcations. Linear theory, nonlinear simulations, and experiments with pure liquids in inclined layers have shown that buoyant longitudinal instabilities (rolls with axis parallel to the slot) are preferred below a critical angle of inclination where shear driven transverse (rolls with axis perpendicular to the slot) convection becomes more critical [1,2]. Binary fluid double-diffusive instabilities have also received considerable attention when thermodiffusional effects are neglected [3].

The theory of convective instabilities driven by a temperature difference imposed on a homogeneous binary mixture contained in a horizontal layer, including the Soret effect, heated from above or below, continues to attract attention [4,5]. The thermodiffusional mass flux creates a vertical concentration gradient that contributes to unstable (stable) stratification if separation is negative (positive) so that the heavier component migrates to the hot (cold) wall. While the heated from above case is double-diffusive unstable with zero wave number when separation is negative [4–7], it has been utilized to measure both positive and negative Soret coefficients [8–10].

A temperature difference imposed on a binary mixture in a vertical slot generates a return buoyant flow, a horizontal Soret mass flux, and hence a vertical concentration gradient. This gradient contributes to unstable (stable) stratification if separation is negative (positive) so that the heavier component migrates to the hot (cold) wall and is convected upward. This forms the basis of the thermogravitational column where the thermodiffusion coefficient is inferred from the measured weak molecular separation along with the equa-

tions that describe the assumed stable steady-state return flow. This weak vertical concentration gradient can be substantially enhanced, thereby improving the measurement accuracy, by inclining the column [11] while heating from above to presumably enhance the stability of the return flow. However, when separation is negative, linear stability analysis of a vertical layer predicts stationary longitudinal convective instabilities with zero wave number driven by diffusion in the direction normal to the imposed temperature gradient at any temperature difference [12] in complete agreement with [13], where the adverse density gradient is imposed on the layer and not as a result of the layer dynamics.

In this paper we investigate the linear stability of the buoyant return flow in a side-heated infinite inclined slot when separation is negative. An asymptotic analysis in the long-wave approximation shows that zero wave number stationary longitudinal convection is triggered at any temperature difference when the layer is not horizontal. A long-wave asymptotic analysis is also performed for a horizontal layer heated from above to determine the critical two-dimensional double-diffusive state. Results of the approximate analyses are confirmed by numerical solutions of the linear stability eigenvalue problem for a particular water-ethanol mixture. Numerical results are also given for the same mixture but assuming negligible Soret effect in order to demonstrate the dramatic influence of negative separation. The transition from stationary longitudinal instabilities in an inclined layer to either overstable convection in a heated from below horizontal layer or to stationary double-diffusive convection in a heated from above horizontal layer is also elucidated and shows that the long-wave regime terminates very close to the horizontal arrangements. Thus the results of this research are important to achieve accurate measurements of the Soret and thermodiffusional coefficients in horizontal, vertical, and inclined layers.

II. FORMULATION

We consider the infinite inclined layer of width l shown in Fig. 1. The isothermal no-slip no-mass flux boundaries are

*zebib@rutgers.edu

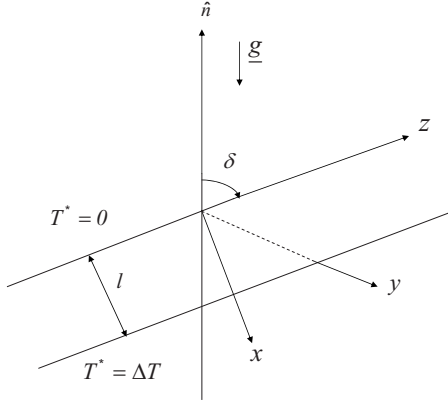


FIG. 1. The model and coordinate system.

maintained at a temperature difference ΔT . We assume linear variation in the density with temperature and concentration of the lighter component,

$$\rho^* = \rho_0 [1 - \alpha(T^* - T_0) - \beta(C^* - C_0)], \quad \alpha > 0, \quad \beta > 0, \quad (1)$$

where starred quantities are dimensional and subscript 0 denotes a reference state. The mass flux can be written in the form [14]

$$\underline{J}^* = -\rho^*(D\nabla C^* + D^T\nabla T^*), \quad (2)$$

where D is the isothermal diffusion coefficient and D^T is the thermodiffusion coefficient. The motion is described in the Cartesian coordinates (x, y, z) of Fig. 1. The variables are scaled with $l, \frac{\kappa}{l}, \frac{l^2}{\kappa}, \Delta T, \frac{\alpha\Delta T}{\beta}$ for length, velocity, time, temperature, and concentration, respectively, where κ is the thermal diffusivity. The nondimensional Boussinesq equations become [12]

$$\nabla \cdot \underline{u} = 0, \quad (3)$$

$$\frac{D\underline{u}}{Dt} = -\nabla p + \text{Pr} \nabla^2 \underline{u} + \text{Pr} \text{Ra}(T + C)\hat{n}, \quad (4)$$

$$\frac{DT}{Dt} = \nabla^2 T, \quad (5)$$

$$\frac{DC}{Dt} = \frac{1}{\text{Le}} \nabla^2 C - \frac{\varepsilon}{\text{Le}} \nabla^2 T. \quad (6)$$

Here the Prandtl number $\text{Pr} = \frac{\nu}{\kappa}$, the Lewis number $\text{Le} = \frac{\kappa}{D}$, the Rayleigh number $\text{Ra} = \frac{g\alpha l^3 \Delta T}{\nu\kappa}$, where ν is the kinematic viscosity. The separation ratio $\varepsilon = \frac{-\beta D^T}{\alpha D} < 0$ is the ratio of the concentration and temperature-driven density gradients in a steady diffusive state and the light component migrates to the hot (cold) wall according to $\varepsilon > 0$ ($\varepsilon < 0$). The boundary conditions at $x=0$ and 1 are

$$\underline{u} = 0, \quad \frac{\partial C}{\partial x} - \varepsilon \frac{\partial T}{\partial x} = 0, \quad (7)$$

$$\text{and } T|_{x=0} = 0, \quad T|_{x=1} = 1. \quad (8)$$

Equations (3)–(8) admit the basic steady return flow [12],

$$T = x, \quad C = f(x) + \gamma z, \quad \underline{u} = W(x)\hat{k}, \quad (9)$$

where \hat{k} a unit z vector and primes denote x derivatives, and along with the global conservation conditions

$$\int_0^1 W dx = 0, \quad \int_0^1 \left(WC - \frac{\gamma}{\text{Le}} \right) dx = 0, \quad (10)$$

we have

$$W = -\psi', \quad f' = \varepsilon - \gamma \text{Le} \psi, \quad (11)$$

and the stream function $\psi(x)$ satisfies

$$\begin{aligned} & \psi^{iv} + \gamma \text{Le} \text{Ra} \cos \delta \psi' - \text{Ra} \{ (1 + \varepsilon) \cos \delta + \gamma \sin \delta \} \\ & = 0, \quad \psi|_{x=0,1} = \psi'|_{x=0,1} = 0, \end{aligned} \quad (12)$$

$$\text{with } H \equiv \int_0^1 \psi dx, \quad K \equiv \int_0^1 \psi^2 dx, \quad \gamma = \frac{\varepsilon H \text{Le}}{1 + \text{Le}^2 K}. \quad (13)$$

Here γ is the induced constant concentration gradient along the layer. Given Ra and γ (or ε) Eqs. (12) and (13) are solved iteratively for ε (or γ). It is noted that $W = \psi = 0$, $\gamma = 0$, and $f' = \varepsilon$ when the layer is horizontal, i.e., $\delta = \pm 90^\circ$.

Linear instability of this basic flow is investigated by assuming perturbations $\{u, v, w, p, \vartheta, \varphi\}(x) e^{i(k_y y + k_z z) + \sigma t}$ for the velocity components, pressure, temperature, and concentration, respectively; k_y and k_z are the longitudinal and transverse wave numbers, respectively (we note here that the terms longitudinal and transverse were unfortunately transposed in [12]). The linear stability equations similar to those in [12] with $d = d/dx$ become

$$du + ik_y v + ik_z w = 0, \quad (14)$$

$$\{\text{Pr}(d^2 - k^2) - ik_z W\}u - dp - \text{Pr} \text{Ra}(\vartheta + \varphi) \sin \delta = \sigma u, \quad (15)$$

$$\{\text{Pr}(d^2 - k^2) - ik_z W\}v - ik_y p = \sigma v, \quad (16)$$

$$\begin{aligned} & \{\text{Pr}(d^2 - k^2) - ik_z W\}w - W'u - ik_z p + \text{Pr} \text{Ra}(\vartheta + \varphi) \cos \delta \\ & = \sigma w, \end{aligned} \quad (17)$$

$$\{(d^2 - k^2) - ik_z W\}\vartheta - u = \sigma \vartheta, \quad (18)$$

$$\left\{ \frac{1}{\text{Le}}(d^2 - k^2) - ik_z W \right\} \varphi - \frac{\varepsilon}{\text{Le}}(d^2 - k^2)\vartheta - f'u - \gamma w = \sigma \varphi, \quad (19)$$

where $k^2 = k_y^2 + k_z^2$ and the boundary conditions at $x=0$ and 1 are

$$u = v = w = \vartheta = d\varphi - \varepsilon d\vartheta = 0. \quad (20)$$

Numerical solutions of Eqs. (14)–(20) are obtained by a Chebyshev pseudospectral method. For each Le , Pr , ε , and δ

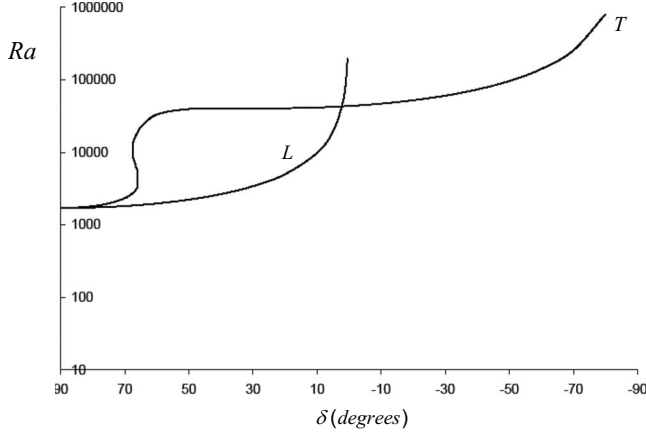


FIG. 2. Stability boundaries with $\varepsilon=0$, $Le=443.8$, $Pr=5.55$. Shown are the transverse (T) and longitudinal (L) with $Ra = \frac{Ra(90^\circ)}{\sin \delta}$ branches.

we calculate the neutral Ra , k_y , k_z , and γ so that $\max\{\text{Re}[\sigma(Ra, k_y, k_z, \gamma; Le, Pr, \varepsilon, \delta)]\} = 0$ in order to delineate the instability region. For each value of Ra the nonlinear algebraic system given by Eqs. (12) and (13) is first solved iteratively for γ , $W(x)$, and $f'(x)$ before the eigenvalues σ are computed. The critical state is determined by minimization of the neutral Ra with respect to k_y and k_z .

III. RESULTS AND DISCUSSIONS

Numerical results will be given for a mixture of 78% water—22% ethanol [15] for which $\varepsilon=-0.118$, $Le=443.8$, $Pr=5.55$. However in order to demonstrate the importance of the Soret effect we also give results for the same mixture but neglecting thermodiffusion, i.e., setting $\varepsilon=0$.

A. Homogeneous water-ethanol mixture with $\varepsilon=0$

In order to show the dramatic influence of thermodiffusion we first display results in Fig. 2 for the same mixture but with $\varepsilon=0$ and hence $\gamma=0$ from Eq. (13). With $k_z=0$ in Eqs. (14)–(20) it follows that $\varphi=0$ so that the longitudinal critical $Ra = \frac{Ra(90^\circ)}{\sin \delta}$ at $k_y=3.11$, where $Ra(90^\circ)=1707.76$. The transverse branch is obtained with $k_y=0$ and again it follows from Eqs. (14)–(20) that $\varphi=0$. It is multivalued S shaped, similar to that for water [16] due to the appearance of disconnected closed neutral curves for $66^\circ \leq \delta \leq 67.5^\circ$. It is also observed that the transverse $Ra \rightarrow \infty$ as heating from above $\delta \rightarrow -90^\circ$, with no species separation, is approached. One notes that the initially homogeneous mixture behaves as a pure liquid in the absence of thermodiffusion with $\varepsilon=0$.

B. Water-ethanol $\varepsilon=-0.118$, $Le=443.8$, $Pr=5.55$

It was shown in [12] that the vertical slot $\delta=0$ is unstable to stationary long wave, $\sigma=0$, longitudinal modes ($k_z=0, k_y \rightarrow 0$) at any $Ra \geq 0$. Here we need to consider the influence of δ on a similar long-wave analysis,

$$-90^\circ < \delta < 90^\circ.$$

With $\sigma=k_z=0$ we assume the expansion

$$(u, v, w, p, \vartheta, \varphi, Ra) = \sum_{n=0}^{\infty} (u_n, v_n, w_n, p_n, \vartheta_n, \varphi_n, R_n) k_y^n, \quad k_y \rightarrow 0, \quad (21)$$

with boundary conditions from Eq. (20) at $x=0$ and 1,

$$u_n = v_n = w_n = \vartheta_n = d\varphi_n - \varepsilon d\vartheta_n = 0. \quad (22)$$

Because diffusion dominates convection when $Ra \rightarrow 0$ it follows from Eq. (13) that

$$\gamma \sim \varepsilon H Le. \quad (23)$$

Moreover the exact solution of Eq. (12) gives (see Eq. (A5) in [12])

$$H \sim Ra \{ (1 + \varepsilon) \cos \delta + \gamma \sin \delta \} \times \left(\frac{1}{720} - \frac{\gamma Le Ra \cos \delta}{4 \times 90 \times 720} + \dots \right), \quad (24)$$

Thus, we have

$$\gamma \sim \frac{\varepsilon \{ (1 + \varepsilon) \cos \delta + \gamma \sin \delta \} Le}{720} Ra. \quad (25)$$

Equations (21) and (25) show that on the neutral curve we also have the expansion

$$\gamma = \sum_{n=0}^{\infty} \gamma_n k_y^n, \quad k_y \rightarrow 0. \quad (26)$$

We now substitute Eqs. (21) and (26) in the linear stability Eqs. (14)–(19). At zeroth order we find using boundary conditions (22),

$$u_0 = v_0 = w_0 = \vartheta_0 = R_0 = \gamma_0 = 0, \quad \varphi_0 = \text{constant}, \quad p_0 = \text{constant}. \quad (27)$$

At first order we find

$$u_1 = \vartheta_1 = 0, \quad \varphi_1 = \text{constant},$$

$$v_1 = \frac{i p_0}{2 Pr} (x^2 - x), \quad w_1 = \frac{-R_1 \varphi_0 \cos \delta}{2} (x^2 - x),$$

$$p_1' = -Pr R_1 \varphi_0 \sin \delta. \quad (28)$$

At second order we obtain $u_2' + i v_1 = 0$ and the two compatibility conditions

$$\int_0^1 v_1 dx = 0 \quad \text{and} \quad \int_0^1 \gamma_1 w_1 dx = \frac{-\varphi_0}{Le}, \quad (29)$$

so that

$$u_2 = v_1 = \vartheta_2 = 0, \quad R_1 = \frac{-12}{\gamma_1 Le \cos \delta}. \quad (30)$$

It can be shown from Eqs. (21) and (25)–(27) that $\gamma_1 = \frac{\varepsilon(1+\varepsilon)Le \cos \delta}{720} R_1$ so that Eq. (30) gives

$$Ra \sim \frac{24}{Le \cos \delta} \sqrt{\frac{-15}{\varepsilon(1+\varepsilon)}} k_y, \quad (31)$$

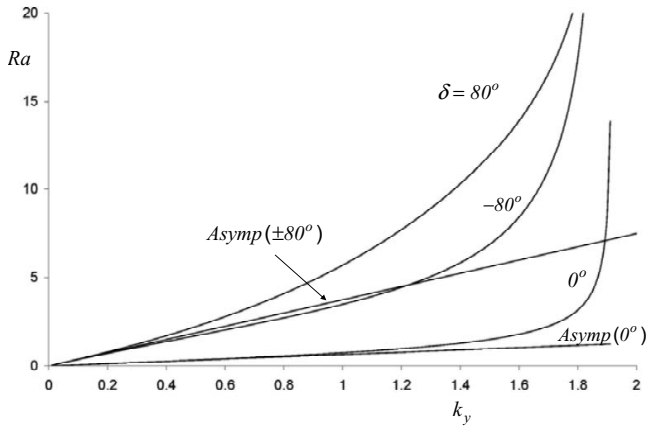


FIG. 3. Neutral curves of longitudinal modes ($k_z=0$) with $\delta = \pm 80$ and 0. Also shown are the asymptotic values from Eq. (31) with excellent agreement as $k_y \rightarrow 0$.

$$\gamma \sim -\sqrt{\frac{-\varepsilon(1+\varepsilon)}{60}}k_y. \quad (32)$$

Full numerical solutions of these longitudinal instabilities are shown in Fig. 3 for $\delta = \pm 80$ and 0. They are indeed found stationary and there is excellent agreement with the asymptotic results of Eqs. (31) and (32) as $k_y \rightarrow 0$ for all $-80 \leq \delta \leq 80$.

Figure 4 gives numerical neutral curves as function of δ for several small values of k_y . Note that Eq. (31) implies symmetry about $\delta=0$ at this order of approximation and that Figs. 3 and 4 are very close to satisfying this symmetry as $k_y \rightarrow 0$.

In the basic state we have from Eqs. (1), (9), and (11)

$$\frac{l}{\alpha \Delta T} \frac{\partial \rho}{\partial n} = -(\nabla T + \nabla C) \cdot \hat{n}, \quad (33)$$

$$= \sin \delta + (\varepsilon - \gamma \text{Le} \psi) \sin \delta - \gamma \cos \delta. \quad (34)$$

It follows that the basic state $\frac{\partial \rho}{\partial n} > 0$ for $\delta \geq 0$ since $\gamma < 0$ and $\psi > 0$ and, hence, the Wooding [14] instability is operative.

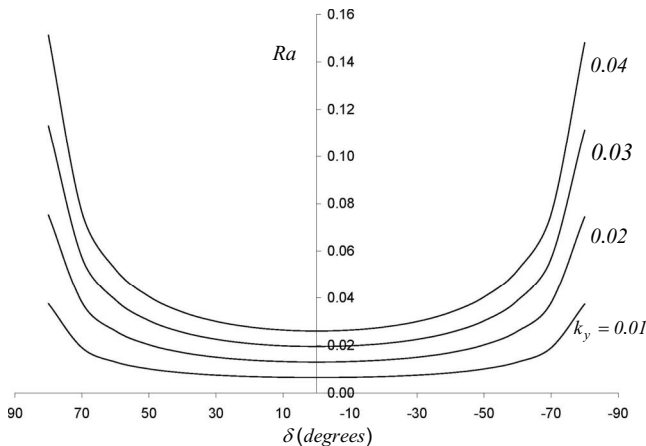


FIG. 4. Stability boundaries of stationary longitudinal modes with $k_z=0$. The flow is unstable for $Ra \geq 0$.

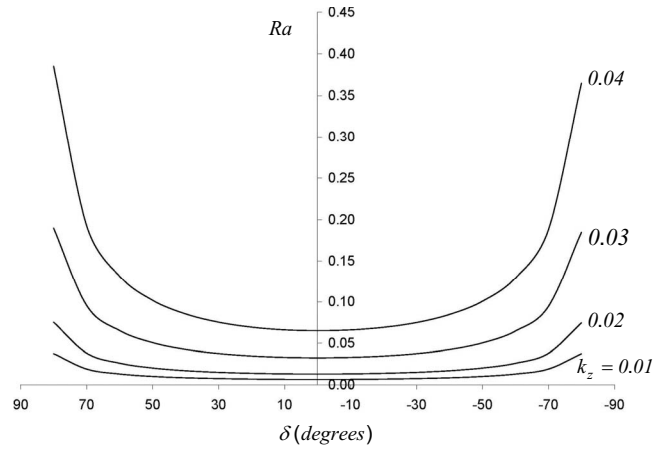


FIG. 5. The stabilizing influence of small transverse components on longitudinal modes with $k_y=0.01$. All branches are stationary.

However $\frac{\partial \rho}{\partial n} < 0$ on the stability boundaries of Fig. 4 for $\delta < 0$ because the temperature contribution, the first term in Eq. (34), overwhelms that by the concentration, the next two terms in the equation. In fact $\frac{\partial \rho}{\partial n} = 0$ on the $k_y=0.01$ stability boundary of Fig. 4 when $\delta \approx -0.03^\circ$. Yet the flow is unstable for $\delta < 0$ to the long longitudinal waves in Fig. 3 and Eqs. (31) and (32). This is because the large Le concentration fluctuations persist while temperature perturbations equilibrate much faster. Thus remarkably the Wooding instability is also operative for $\delta < 0$.

The transverse modes are more stable and their stabilizing influence on the longitudinal instabilities with $k_y=0.01$ is shown in Fig. 5. In comparison with Fig. 2 with zero separation, the $\varepsilon < 0$ thermodiffusional instabilities in Figs. 3–5 cannot be suppressed and are triggered at $Ra \geq 0$,

$$\delta = -90^\circ.$$

The heated from above case $\delta = -90^\circ$ is doubly-diffusive unstable at zero wave number [4–7]. Accordingly we set $\sigma = k_z = W = \gamma = 0$ so that $w = 0$ (because this instability is two

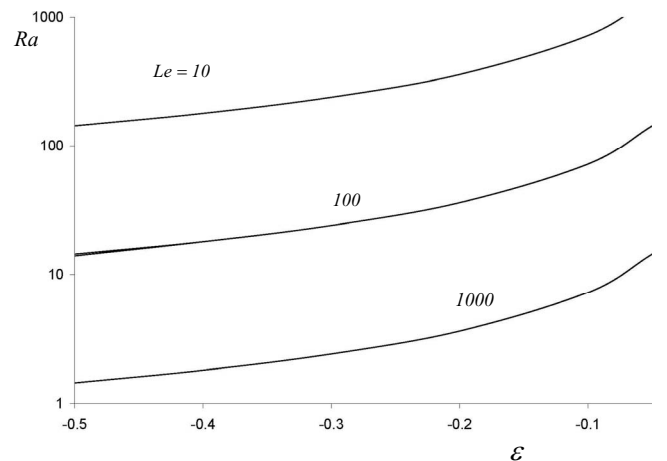


FIG. 6. Stability boundaries for heating from above with $\delta = -90^\circ$, $k_z=0$, and $k_y=0.001$. The asymptotic values given by Eq. (38) are indistinguishable from the numerical ones on these scales.

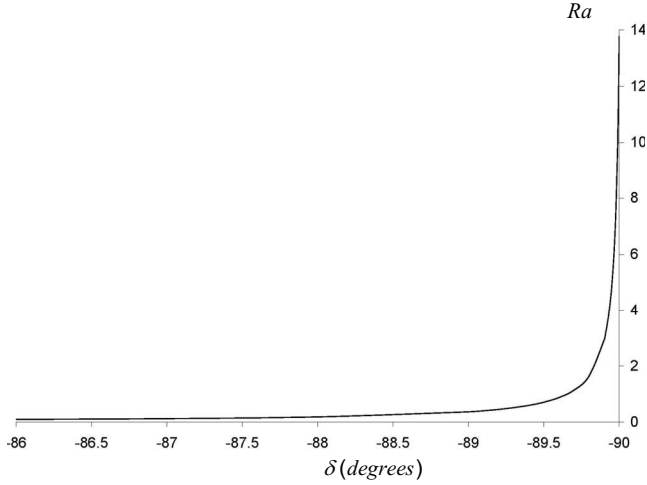


FIG. 7. Stability boundary with $k_z=0$ and $k_y=0.01$ showing the merger of the two stationary long-wave instabilities given asymptotically by Eqs. (31) and (38).

dimensional we can proceed with $\sigma=k_y=v=0$). We assume the same expansion and boundary conditions given by Eqs. (21) and (22). At zeroth order Eqs. (14)–(19) give

$$u_0 = v_0 = \vartheta_0 = 0, \quad \varphi_0 = \text{constant}, \quad p'_0 = \text{Pr} R_0 \varphi_0. \quad (35)$$

At first order we find

$$u_1 = \vartheta_1 = 0, \quad \varphi_1 = \text{constant}, \quad v''_1 = \frac{ip_0}{\text{Pr}}. \quad (36)$$

At second order we obtain $u'_2 + iv_1 = 0$ and the two compatibility conditions

$$\int_0^1 v_1 dx = 0 \quad \& \quad \int_0^1 \varepsilon u_2 dx = \frac{-\varphi_0}{\text{Le}}. \quad (37)$$

Thus from Eqs. (35) and (36) we find $v_1 = iR_0 \varphi_0 (\frac{x^3}{6} - \frac{x^2}{4} + \frac{x}{12})$ and $u_2 = \frac{R_0 \varphi_0}{24} (x^4 - 2x^3 + x^2)$ so that

$$\text{Ra} \sim \frac{-720}{\varepsilon \text{Le}}, \quad k_z = 0, \quad k_y \rightarrow 0. \quad (38)$$

This asymptotic value is also valid with $k_y=0$ and $k_z \rightarrow 0$. Figure 6 shows numerical stability boundaries with $k_z=0$ and $k_y=0.001$ as functions of ε and Le . Also shown are the asymptotic values given by Eq. (38) that are seen to be indistinguishable on the scales of the figure. These results are also in excellent agreement with [5,17].

Full numerical solution with $k_z=0$ and $k_y=0.01$ is given in Fig. 7 and shows how the two asymptotic solutions in Eq. (31) and (38) merge near $\delta=-90^\circ$,

$$\delta = 90^\circ.$$

Finally heating from below with $\delta=90^\circ$ [4,5] is stabilized relative to ordinary Rayleigh-Benard convection and is overstable at $\text{Ra} \approx 1923.6$; $k_y \approx 3.13$ and $k_z=0.0$ (or $k_y=0.0$ and

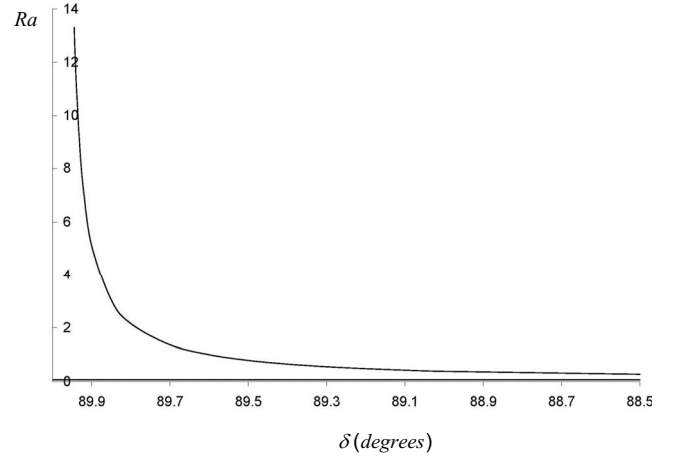


FIG. 8. Stability boundary with $k_z=0$ and $k_y=0.01$ showing the end of the stationary long-wave regime Eq. (31) near $\delta=90^\circ$.

$k_z \approx 3.13$); $\sigma_i \approx 6.92$. Full numerical solution near $\delta=90^\circ$ is shown in Fig. 8 where the stationary long-wave regime is seen to end at $\delta \approx 89.95^\circ$.

IV. CONCLUDING REMARKS

A linear stability study of the thermodiffusional driven return flow of a binary fluid with negative separation in a side-heated infinite inclined layer was performed. Results from both numerical solutions and long-wave approximations when $\delta \neq 90^\circ$ are in excellent agreement. It is shown that the critical Ra for these long-wave longitudinal instabilities is zero. The heated from above case $\delta=-90^\circ$ is doubly-diffusive unstable since the $\text{Le} > 1$. The zero wave number, stationary, and longitudinal Wooding instabilities at zero Ra are present when $\delta \neq \pm 90^\circ$. This is because the basic steady return flow is unstably stratified with $\frac{\partial p}{\partial n} > 0$ when $90^\circ > \delta \geq 0^\circ$. They are also present even if it is stably stratified with $\frac{\partial p}{\partial n} < 0$ when $0^\circ < \delta < -90^\circ$ thanks to the double-diffusive mechanism that diminishes the influence of the stabilizing temperature relative to the destabilizing concentration perturbations.

The asymptotic Eqs. (31) and (38) giving, respectively, critical values of Ra for an inclined layer and a heated from above horizontal layer should be very helpful to experimentalists when designing thermogravitational columns and Soret cells.

An important conclusion of the present work is that the Soret effect cannot be ignored no matter how small is the negative separation. The implication of our results to thermogravitational columns and Soret cells of finite extent in the x and y directions needs to be investigated by direct simulations of the full nonlinear three-dimensional time-dependent equations.

ACKNOWLEDGMENTS

This research is supported by the Ikerbasque Foundation and the project GOVSORET (Grant No. PI 2008-14).

- [1] E. Bodenschatz, W. Pesch, and G. Ahlers, *Annu. Rev. Fluid Mech.* **32**, 709 (2000).
- [2] K. E. Daniels, B. B. Plapp, and E. Bodenschatz, *Phys. Rev. Lett.* **84**, 5320 (2000).
- [3] J. S. Turner, *Annu. Rev. Fluid Mech.* **17**, 11 (1985).
- [4] R. S. Schechter, M. G. Velarde, and J. K. Platten, *Adv. Chem. Phys.* **26**, 265 (1974).
- [5] B. Huke, H. Pleiner, and M. Lucke, *Phys. Rev. E* **78**, 046315 (2008).
- [6] A. La Porta and C. M. Surko, *Phys. Rev. Lett.* **80**, 3759 (1998).
- [7] R. Cerbino, A. Vailati, and M. Giglio, *Phys. Rev. E* **66**, 055301(R) (2002).
- [8] P. Kolodner, H. Williams, and C. Moe, *J. Chem. Phys.* **88**, 6512 (1988).
- [9] K. J. Zhang, M. E. Briggs, R. W. Gammon, and J. V. Sengers, *J. Chem. Phys.* **104**, 6881 (1996).
- [10] J. K. Platten, *J. Appl. Mech.* **73**, 5 (2006).
- [11] J. K. Platten, M. M. Bou-Ali, and J. F. Dutricux, *J. Phys. Chem.* **107**, 11763 (2003).
- [12] A. Zebib, *J. Chem. Phys.* **129**, 134711 (2008).
- [13] R. A. Wooding, *J. Fluid Mech.* **7**, 501 (1960).
- [14] K. B. Haugen and A. Firoozabadi, *J. Chem. Phys.* **122**, 014516 (2005).
- [15] M. M. Bou-Ali, O. Ecenarro, J. A. Madariaga, C. M. Santamaria, and J. J. Valencia, *Phys. Rev. E* **62**, 1420 (2000).
- [16] Y.-M. Chen and A. J. Pearlstein, *J. Fluid Mech.* **198**, 513 (1989).
- [17] E. Knobloch and D. R. Moore, *Phys. Rev. A* **37**, 860 (1988).